



Tailoring the emission of Eu based hybrid materials for light-emitting diodes application

Xianli Lu^a, Dongming Cheng^{a,*}, Fuying Dong^{a,c}, Shirong Qin^a, Yachuan Liang^a, Yingjie Lu^a, Qian Liu^a, Chongxin Shan^{a,b,*}, Lin Dong^{a,*}

^a School of Physics & Engineering, Zhengzhou University, Zhengzhou 450052, China

^b State Key Laboratory of Luminescence and Applications, Changchun Institute of Optics, Fine Mechanics and Physics, Chinese Academy of Sciences, Changchun 130033, China

^c Zhengzhou No. 1 High School, Zhengzhou 450001, China

ARTICLE INFO

Keywords:

Phosphor

SrAl₂O₄:Eu

EA(TTA)₃phen

Tunable color rendering

ABSTRACT

The rare-earth elements (REEs) derived phosphors play an essential role in light-emitting diodes. Many approaches have been proposed for tailoring the emission color of lamp phosphors by tuning the contents and valences of REEs (such as Ce³⁺, Tb³⁺, Eu³⁺). As we know, the separation and purifying of REEs from waste phosphors usually requires high cost and complicated operations. Here we report the phosphor only based on Eu doped in different matrices with manipulated color for the first time, which will minimize the environmental challenges present in the transition to a green economy. The hybrid material is manufactured by mixing (SAOE) SrAl₂O₄:Eu²⁺ and (TTAE) Eu(TTA)₃phen (TTA = 2-thenoyltrifluoroacetone, phen = 1,10-phenanthroline) in different mass ratios. The optical properties of the resulting phosphor materials are determined by photoluminescence (PL). Eu doped in alkaline earth aluminates (SrAl₂O₄) has strong green (510 nm) emission, meanwhile the Eu exhibits enhanced red (612 nm) luminescence upon bonding with TTA (thenoyltrifluoroacetone) and phen ligands. By adjusting the mass ratios of SAOE and TTAE, the emission colors of the hybrid materials can be tuned from red to green. The chromaticity coordinates are calculated, which fell well in the red, orange, yellow and green regions of 1931 CIE chromaticity diagram. According to the spectroscopic studies, the absorption almost have no overlap on the emissions of SAOE and TTAE powders, leading to efficient PL emitting with high photoluminescence quantum yields of 24–68%. Through deposition of the hybrid materials with polydimethylsiloxane (PDMS) onto the 365 nm UV-LED chip, tunable color light-emitting diodes are fabricated, they show excellent luminescence properties, indicating their potential application in optical device and offering a novel approach for designing multi-color phosphor materials.

1. Introduction

Phosphors with well-tailored emitting wavelength have aroused extensive research interests for their multitudinous applications in light conversion, radiation detector and visual displays. Especially, rare-earth elements (REEs) derived phosphors account for the major part of the total commercial consumption of phosphors. REEs phosphors have been widely utilized for lamps and display devices [1], optical telecommunication [2], light emitting diodes (LEDs) [3], novel optoelectronic devices [4] and biological labels [5] for their unique merits: (a) strong and sharp line-like emission, (b) high photo-stability, (c) large Stokes shift, and (d) long-lived excited states [6]. Usually, multiple REEs are incorporated in the same phosphor to achieve bright emission with desired CIE color coordinates, e.g., Ce³⁺, Tb³⁺, Eu³⁺ co-doped

phosphors to achieve manipulated color emission as excited by UV LED chips [7,8].

However, the reserves of REEs on the earth are very limited, and the mining and purifying of rare earths requires high cost and complicated operations [9]. To recycle REEs from waste phosphors is regarded as one of the potential solutions for the problem of REEs supplies. Unfortunately, the recycling of REEs by means of pneumatic classification, leaching treatment and oxalate precipitation requires complexed long treatment. Further separation and purifying of REEs from the recycled coarse mixtures of multiple REEs requires even more refinery process, and causes the major part of expensive cost and environmental burden [10]. As a result, only less than 1% of the REEs containing waste phosphors were actually recycled, according to Binnemans' comprehensive review [11]. Thus it is meaningful to develop REEs phosphors

* Corresponding authors at: School of Physics & Engineering, Zhengzhou University, Zhengzhou 450052, China.

E-mail addresses: chengdm@zzu.edu.cn (D. Cheng), cxshan@zzu.edu.cn (C. Shan), ldong@zzu.edu.cn (L. Dong).

with single rare earth element and tunable emission colors, which will avoid the complicated refinery process and promise the efficient exploitation of REEs waste phosphors.

The luminescence of europium is very strongly dependent on the host lattice [12]. The emission of Eu is due to the optical transitions within the f-manifolds [13]. The f-electrons are well shielded from the chemical environment and therefore have almost retained their atomic character [14,15]. One of the most interesting Eu^{2+} doped materials is SrAl_2O_4 which proves to be an efficient host material and offers the possibility of generating broad band green emissions (510 nm) attributed to its $4f^65d \rightarrow 4f^7$ transition [16]. Meanwhile, Eu^{3+} doped materials, especially in which the Eu ion occupies a non-centrosymmetric site, have been widely used as the red-emitting phosphors due to their intense $^5\text{D}_0 \rightarrow ^7\text{F}_2$ emission in the red spectral region [17,18]. Eu^{3+} exhibits enhanced red (612 nm) luminescence upon bonding with TTA (2-thenoyltrifluoroacetone) and phen (1,10-phenanthroline) which together served as organic ligands to chelate RE ions and transfer exciting light to the RE ions efficiently [19]. In this luminescence sensitization process, the organic ligand with strong optical absorption is first excited under the excitation wavelength, and then the absorbed energy is transferred to the associated Eu ion which results in efficient emission [20]. Therefore, we may tailor the emission color by combining these phosphors with uni-REEs.

In this paper, a simple and convenient synthetic method was put forward to synthesize uni-REE phosphors with tunable emission color from red to green, by adjusting the mass ratios of SAOE and TTAE. The as-synthesized hybrid materials with tunable CIE coordinates were encapsulated on the UV-chip (365 nm, 1 W) to fabrication multi-color LEDs. These results may realizing multi-color emission phosphors by one single rare earth element, and can be readily extended to other REEs phosphors beyond europium. This may pave a way for feasible recycling REEs containing wastes with reduced economic and environmental costs.

2. Experimental

2.1. Chemicals

The aluminum oxide (Al_2O_3), Strontium carbonate (SrCO_3), boracic acid (H_3BO_3), triethylamine ($(\text{CH}_3\text{CH}_2)_3\text{N}$), 2-thenoyltrifluoroacetone (TTA) and 1,10-phenanthroline (phen) were purchased from Aladdin Chemistry Co. Ltd. (Shanghai, China). Europium oxide (Eu_2O_3) were purchased from Beijing HWRK Chem Co. Ltd. (Beijing, China). Ethyl alcohol absolute ($\text{C}_2\text{H}_5\text{OH}$) was purchased from Tianjin Yong Da Chemical Reagent Co. Ltd. (Tianjin, China). Hydrochloric acid (HCl) were purchased from Luoyang Chemical Reagent. (Luoyang, China). All the reagents were of analytical grade and were used without further purification.

2.2. Synthesis of SAOE and TTAE

The SAOE particles were prepared via a solid-state reaction at high temperature following a modified literature procedure [21]. Appropriate amount of raw materials including Al_2O_3 , H_3BO_3 , SrCO_3 , and Eu_2O_3 powders (typically 1 mol% H_3BO_3 flux, 0.5 mol% Eu_2O_3 and 99 mol% SrCO_3 with respect to Al_2O_3 , e.g., 0.0618 g H_3BO_3 flux, 0.1760 g Eu_2O_3 , 14.6150 g SrCO_3 and 10.1960 g Al_2O_3 was used for a typical synthesis) were thoroughly mixed by wet grinding for 2 h, with ethanol as the dispersion medium. The mixture was transferred into the thermostat oven and dried for 1 h at 70 °C. Then the dried powder mixture was loaded into a corundum crucible and pre-fired at 900 °C in the air for 1 h. After naturally cooled down to the room temperature, the pre-fired product was grounded again, and sintered at 1300 °C for another 4 hrs in a reducing atmosphere with a flow of Ar and 5% H_2 gases. Finally the sintered product was grounded again into powders for subsequent characterizations and use.

The TTAE was synthesized by wet chemical route [22]. First, Eu_2O_3 was dissolved in hydrochloric acid with vigorous magnetic stirring at 80 °C until the EuCl_3 crystal separated out. The coarse EuCl_3 precipitates were re-dissolved in ethanol, and the solution was kept heating to evaporate residue acid until its pH reaches above 6.5. Appropriate amount of ethanol was then added to obtain a clear stock solution with 0.5 mol/L EuCl_3 . To synthesize the TTAE, 2-thenoyltrifluoroacetone (3 mmol), 1,10-phenanthroline (1 mmol) and 2 mL of triethylamine were dissolved in 15 mL of ethanol to obtain a solution of the ligands. Then, 2 mL of EuCl_3 solution (0.5 mol/L, 1 mmol) was added dropwise under constant stirring. During this process, a white precipitate of the TTAE complex was formed. Afterwards, the precipitate was collected by centrifugation with 6000 rpm for 10 min, and then dried in a blast drying oven at 60 °C for 2 h.

2.3. Preparation of phosphors with tailored color

In order to obtain phosphors with various emission color, the TTAE and SAOE powders with the weight ratios of 1:0, 1:25, 1:50, 1:100, 1:200, 1:300, 1:400, 0:1 was mixed and grinded for 30 min to form a homogeneous fine powder. The resultant samples were denoted as P-A (pure TTAE), P-B, P-C, P-D, P-E, P-F, P-G, P-H (pure SAOE), respectively.

2.4. Fabrication of phosphor-based LEDs and luminescent blocks

The UV LED chips with an emission centered at 365 nm were utilized as excitation sources. The as synthesized P(A-H) phosphors were admixed with polydimethylsiloxane (PDMS), vacuumed to expel the gas bubble, and then dropped on commercial UV chips. The phosphors covered LEDs were dried at 70 °C for 5 h. We also fabricate the phosphor-based luminescent blocks. The P(A-H) were added to the polydimethylsiloxane (PDMS) under mechanical stirring for 20 min. The mixtures were poured into specific mold and cured. Then phosphor-based luminescent blocks were obtained after removing from the mold.

2.5. Characterization

The X-ray diffraction (XRD) pattern of SAOE was recorded using an X'Pert Pro diffractometer, in which X-rays were generated by a Cu K α source. The morphology of the sample was observed by SEM (JSM-6700F, JEOL). EDS were conducted on Oxford Instruments. The composition of the materials was recorded by X-ray photoelectron energy spectra (XPS) using a Thermo Scientific Escalab 250Xi with Al K α radiation. The PLQYs and fluorescence spectra of the SAOE and TTAE were obtained with an F-7000 fluorescence spectrophotometer manufactured by Hitachi. The UV–Vis absorption of the SAOE and TTAE were obtained with a UH4150 spectrophotometer. Fourier transform infrared (FTIR) spectra of the samples were recorded on a Thermo Scientific NicolettiS10 FTIR spectrometer, over the range 4000–400 cm^{-1} .

3. Results and discussion

3.1. Structure of SAOE and TTAE

In this work, a facile and general strategy was developed to synthesize SAOE and TTAE. All the diffraction peaks in the XRD pattern of the SAOE powder were in good agreement with those of monoclinic SrAl_2O_4 (JCPDF card No. 00-034-0379), and no impurity peaks were observed, as shown in Fig. 1(a). Since europium is of the same valence and very similar radius (0.117 nm) to strontium (0.118 nm) [23], Sr^{2+} is readily substituted by Eu^{2+} [24]. The morphology of the as-synthesized SAOE powder is characterized by scanning electron microscopy (SEM), as presented in Fig. 1(b). Dispersed conglomerates have been obtained with the mean size of 3.04 μm , as calculated in the inset of Fig. 1(b). A peak of Eu is observed in the energy dispersive spectrum of

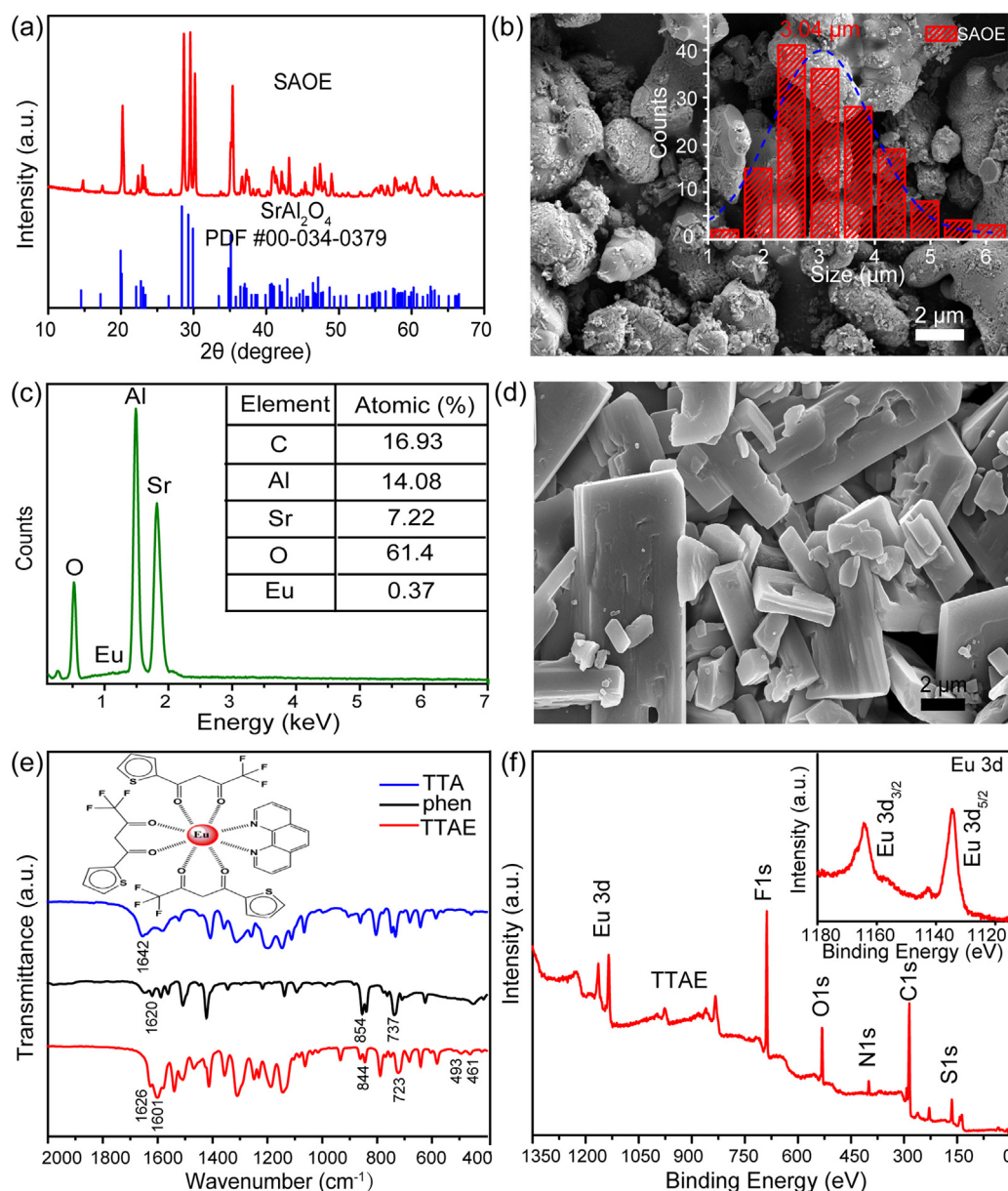


Fig. 1. (a) XRD patterns of SAOE. (b) SEM images of SAOE. (c) EDX spectrum of the SAOE. Insert: Element content of SAOE. (d) SEM images of TTAE. (e) FTIR spectra of the TTAE and the ligands. Inset: The structure of TTAE. (f) XPS survey scan and Eu 3d core level spectra of TTAE.

Table 1

Elemental analysis results of the TTAE observed by X-ray photoelectron spectroscopy.

Sample	Elemental atomic percentage (%)					
	C	N	S	F	Eu	O
P-A	58.83	3.50	5.49	18.55	2.65	10.98

SAOE shown in Fig. 1(c), confirming the existence of the element Eu in the sample. The peak is relatively weak because of the low doping concentration of Eu. The atomic concentrations of the SAOE are determined by XPS, as shown in insert of Fig. 1(c). On the basis of calculations made for $\text{Sr}_{99}\text{Al}_{2}\text{O}_{4}:\text{Eu}_{01}$ compound, the ratio of Sr:Al:O:Eu is 8.7:16.95:73.91:0.44, in well accordance with the composition of the starting materials [25].

The morphology of the as-synthesized TTAE powder is characterized by scanning electron microscopy (SEM), as presented in Fig. 1(d).

The TTAE particles have cuboid-like structure. FTIR spectroscopy is carried out to confirm the formation of the TTAE complex, as shown in Fig. 1(e). The peak at 1620 cm^{-1} which corresponding to the characteristic stretching vibration of C=N of free phen molecules shifts to 1601 cm^{-1} of when they are bonded with Eu^{3+} . And the C-H bending peaks appear at 737 and 854 cm^{-1} of free phen both shift to lower frequencies at 723 and 844 cm^{-1} , respectively. It certifies the co-ordination of Eu^{3+} with phen [26]. Compared with TTA, two additional peaks are observed at 493 and 461 cm^{-1} in the spectra of the TTAE, which is attributed to the stretch vibration of the $\text{Eu}\leftarrow\text{O}$ coordination bond [27], suggesting a strong interaction exists between TTA ligand and europium for the formation of the stable chelate ring. Also, the FTIR peak at 1642 cm^{-1} , which is attributed to the stretching vibration of C=O of TTA, exhibits a slight bathochromic shift to 1626 cm^{-1} as for TTAE, because of the attenuation of C=O vibration during the formation of $\text{Eu}\leftarrow\text{O}$ coordination bond [28]. The molecular structure of TTAE is shown in insert of Fig. 1(e).

Furthermore, XPS measurement was carried out to analyze the

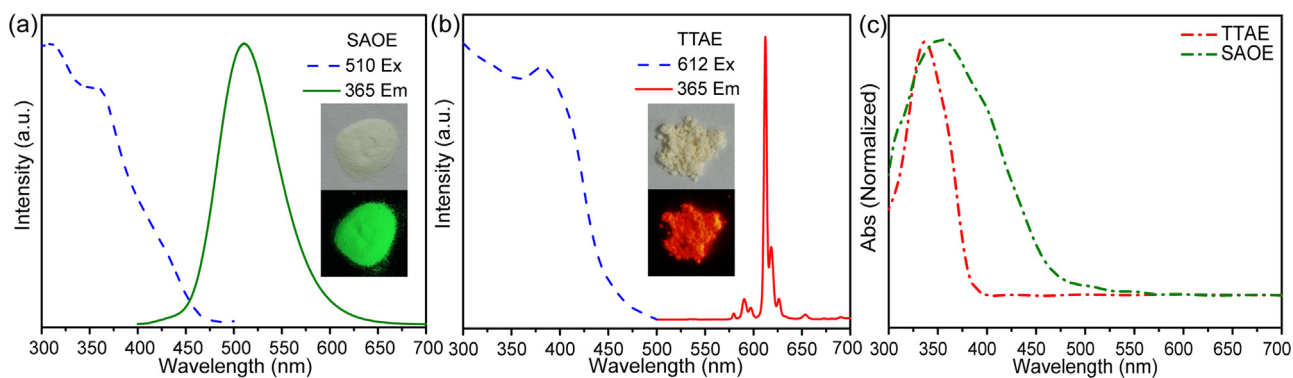


Fig. 2. (a) The excitation spectrum (dot line) and emission spectrum (green solid line) of the SAOE. (b) The excitation spectrum (dot line) and emission spectrum (red solid line) of the TTAE. Insets: photographs of SAOE and TTAE under indoor illumination condition and UV irradiation. (c) UV-Vis absorption spectra of SAOE (green) and TTAE (red).

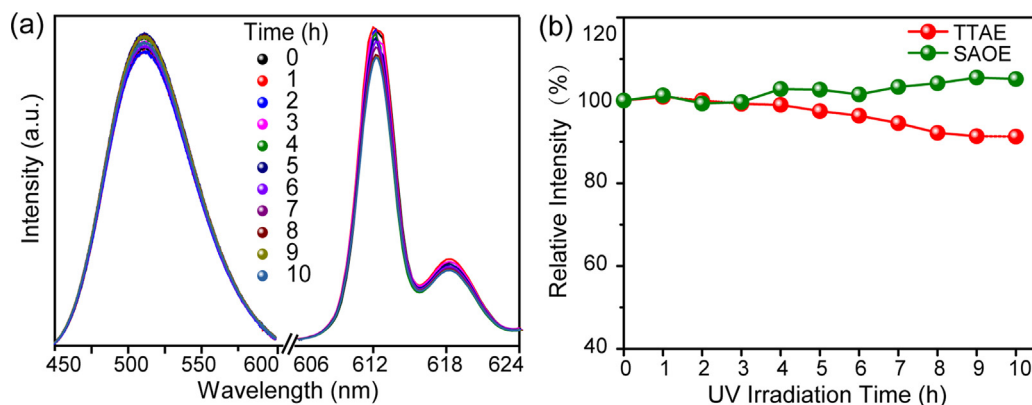


Fig. 3. (a) Emission spectra of SAOE and TTAE measured at different irradiation time. (b) Relative emission intensity versus the irradiation time under 365 nm UV light of SAOE and TTAE.

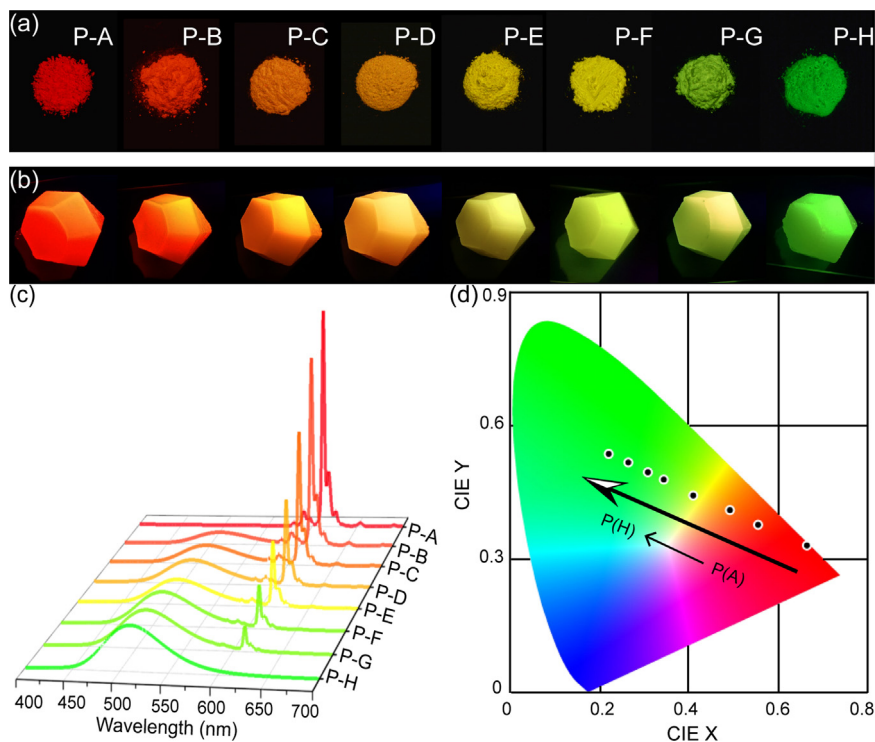


Fig. 4. (a) Luminescence images under 365 nm UV light of composite: (a) phosphors P-A, P-B, P-C, P-D, P-E, P-F, P-G, P-H; (b) the phosphors/PDMS composites cast into different shapes (c) The phosphors corresponding emission spectra. (d) CIE chromaticity diagram of the hybrid materials.

Table 2

Mass ratio (TTAE: SAOE), PLQYs at the optimal wavelength excitations and CIE coordinates (x, y) of P(A-H) samples.

Sample	Mass ratio TTAE: SAOE	PLQY λ_{ex} 365 nm	CIE (x,y)
P-A	1:0	24%	(0.662, 0.336)
P-B	1:25	26%	(0.553, 0.385)
P-C	1:50	28%	(0.495, 0.412)
P-D	1:100	35%	(0.409, 0.451)
P-E	1:200	36%	(0.334, 0.482)
P-F	1:300	40%	(0.308, 0.495)
P-G	1:400	55%	(0.263, 0.517)
P-H	0:1	68%	(0.210, 0.542)

surface chemical composition of the TTAE, as shown in Fig. 1(f). The peaks at 165.00, 284.92, 399.64, 532.08 and 688.07 eV are ascribed to S 2p, C 1s, N 1s, O 1s and F 1s, respectively [29,30]. Hence, the TTAE compound contains the element C, N, O, S, F and Eu. The high-resolution spectrum of Eu 3d is shown in inset in Fig. 1(f), in which the peaks located at 1164.32 and 1134.47 eV stem from the spin-orbit splitting of Eu 3d_{3/2} and 3d_{5/2}, respectively [31]. The atomic concentrations of the TTAE are shown in Table 1. The XPS results further confirm the composition of TTAE, which is in good agreement with FTIR results.

3.2. Luminescence performance of SAOE and TTAE

The fluorescence spectra of the SAOE and TTAE powders under UV radiation at 365 nm are shown in Fig. 2(a) and (b), respectively. For the SAOE powder, the fluorescence spectrum of the as-prepared sample are dominated by a broad peak centered at around 510 nm, which can be attributed to the 4f⁶5d → 4f⁷ transition [32]. The photographs of SAOE sample w/o and with 365 nm UV lamp radiation are shown in inset of Fig. 2(a). The SAOE powders are white in color under indoor illumination condition, and show a strong green fluorescence under UV irradiation.

The excitation spectrum for TTAE sample was obtained by monitoring the characteristic emissions of the Eu at 612 nm. As presented in Fig. 2(b), the broad excitation band extending from 300 to 450 nm appears, which is assigned to the π - π^* electronic transitions of TTA organic ligand. The emission spectrum of the TTAE composes of a set of

lines peaking at 578, 591 and 612 nm, which can be ascribed to the electric-dipole $^5D_0 \rightarrow ^7F_J$ ($J = 0, 1, 2$) transitions [26]. The luminescent peak at 612 nm is dominant and in charge of the bright intense red emission (inset of Fig. 2(b)) under UV-light irradiation with 365 nm. The photoluminescence spectrum further confirms ligands have been coordinated with Eu³⁺ and sensitized the activator ions greatly through ‘antenna effect’ [33]. Upon coordination with Eu³⁺, the ligands can absorb excitation energy efficiently and transfer to the Eu³⁺ subsequently due to well-matched energy level between the triplet state of the ligand and the lowest excitation state of Eu³⁺ [34].

The red curve in Fig. 2(c) shows the absorption spectrum of the Eu (TTA)₃phen compound (0.003 g in 3 mL of ethanol and diluted to 1:100) in the 300–700 nm spectral range. For the green curve in Fig. 2(c) shows the diffuse reflectance absorption of SAOE phosphor powders. The UV–Vis absorption spectra of SAOE and TTAE phosphors display an obvious excitonic absorption band peaked at about 353 and 336 nm, respectively. Notably, the self-absorption of SAOE and TTAE is negligible for the lack of overlap between excitonic absorption and emission spectrum, which is beneficial for efficient fluorescence emission. Both SAOE and TTAE exhibit strong emission under irradiation at around 365 nm, indicating that the SAOE and TTAE can be efficiently excited by the UV LED chip at 365 nm, which lays a solid ground for the application of the composite as fluorescent phosphors for UV-chip-based LEDs.

Photostability is a vital indicator for phosphors used in LEDs, thus the photostability of the SAOE and TTAE powders are analyzed by continuously direct exposure to 365 nm UV light (irradiation intensity 0.15 mW/cm²) for 10 h. Obviously, all the time-dependent emission spectra (Fig. 3a) keep almost the same line shape within long time-scale irradiation. The intensity decay curves of SAOE and TTAE have been calculated, as shown in Fig. 3(b). The emission intensity only decreases slightly and maintained around 90% of the initial value even after UV radiation for 10 hrs, indicating the good photo-stability of the SAOE and TTAE powders. Hence, the SAOE/TTAE composite phosphors can be used as down-conversion layer for multi-color LEDs.

Thus, it can be concluded that tunable light emission can be achieved by controlling the mass ratios of SAOE and TTAE emitting components. As shown in Fig. 4(a), we prepared phosphors with emission from green to red by mixing SAOE and TTAE. It shows fluorescence images of these phosphors under 365 nm UV light, whose emissions are blue-shifted from red to green for the samples P-A to P-H.

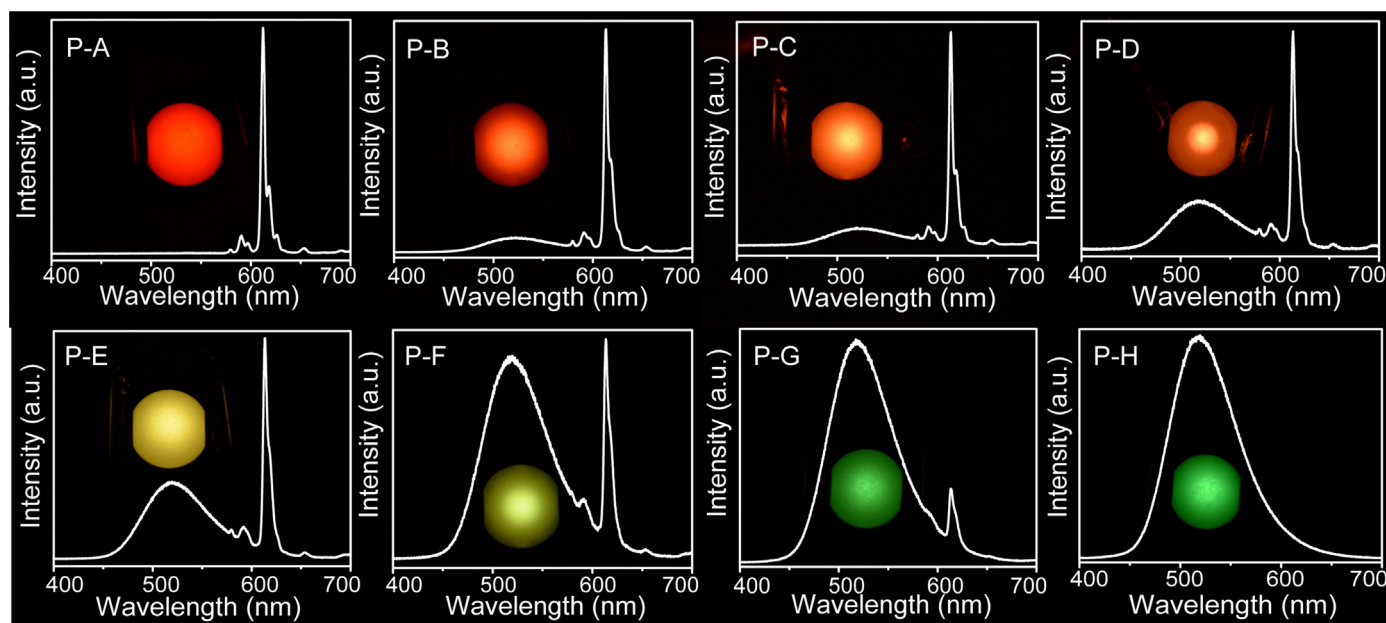


Fig. 5. The photos and emission spectra of multi-color LEDs operating under the voltage of 3.0 V.

The luminescent blocks with specific shape can be easily composed by mixing phosphors in PDMS, as shown in Fig. 4(b), which can be employed as color converters in down-conversion LEDs. Fig. 4(c) shows that the emission spectra of the phosphors. Furthermore, the chromaticity coordinates of the hybrid materials were calculated, which fell well in the red, orange, yellow and green regions of 1931 CIE chromaticity diagram, the CIE color coordinates shift from (0.66, 0.33) to (0.21, 0.54), as shown in Fig. 4(d). The resulting powders P(A-H) show bright emission under UV irradiation with the PLQYs depending on the mass ratios of the constituents: 24% for pure TTAE, 35% for TTAE:SAOE of 1:100 and 68% for pure SAOE at 365 nm excitation, as shown in Table 2.

Based on the above results, the SAOE/TTAE composite phosphors were applied as color conversion layers for LEDs with tunable color rendering. The device was fabricated by embedding the dual-emitting powders in PDMS on a UV diode chip (365 nm, 1 W). Fig. 5 shows the photographs of multi-color LEDs (devices with SAOE/TTAE composite phosphors) under the driven voltage of 3.0 V. Bright light ranging from red to green can be achieved by adjusting the mass ratio of the composite phosphors.

4. Conclusions

In summary, luminescent hybrid materials were synthesized by incorporating Eu in TTA ligand and SrAl_2O_4 matrix. The emission colors of the as-prepared phosphors could be simply tuned from red to green by varying the mass ratio of SAOE and TTAE. The hybrid composites show high photoluminescence quantum yields of 24–68% with good photostability under UV irradiation (365 nm, 0.15 mW/cm^2). The phosphors had been packaged onto a 365 nm UV chip as a multi-color conversion layer of LEDs. The only Eu based hybrid materials with color-tunable and high photoluminescence quantum yields have promise in the lighting field and will pave a way for feasible recycling REEs containing wastes with reduced economic and environmental costs.

Acknowledgements

This work is financially supported by the National Natural Science Foundation of China (U1704138, 11674290, 21601159, 51602288, 61604132) and the National Science Foundation for Distinguished Young Scholars of China (61425021).

References

- Y. Liu, Y. Zhao, H. Luo, Z. Wu, Z. Zhang, Hydrothermal synthesis of CeF_3 nanocrystals and characterization, *J. Nanopart. Res.* 13 (2011) 2041–2047.
- J.-C.G. Bünzli, C. Piguet, Taking advantage of luminescent lanthanide ions, *Chem. Soc. Rev.* 34 (2005) 1048–1077.
- A. Koizumi, Y. Fujiwara, A. Urakami, K. Inoue, Room-temperature electroluminescence properties of Er,O-codoped GaAs injection-type light-emitting diodes grown by organometallic vapor phase epitaxy, *Appl. Phys. Lett.* 83 (2003) 4521–4523.
- M. Aleshina, S. Sivakumar, M. Venkataraman, A.G. Brolo, F.C.J.M. v. Veggel, Significant suppression of spontaneous emission in SiO_2 photonic crystals made with Tb^{3+} -doped LaF_3 nanoparticles, *J. Phys. Chem. C* 111 (2007) 4047–4051.
- R. Kumar, M. Nyk, T.Y. Ohulchanskyy, C.A. Flask, P.N. Prasad, Combined optical and MR bioimaging using rare earth ion doped NaYF_4 nanocrystals, *Adv. Funct. Mater.* 19 (2009) 853–859.
- D. Zhang, Q. Zhao, J. Zang, Y.-J. Lu, L. Dong, C.-X. Shan, Luminescent hybrid materials based on nanodiamonds, *Carbon* 127 (2018) 170–176.
- T. Wang, P. Li, H. Li, Color-tunable luminescence of organoclay-based hybrid materials showing potential applications in white LED and thermosensors, *ACS Appl. Mater. Inter.* 6 (2014) 12915–12921.
- Y. Wada, M. Sato, Y. Tsukahara, Fine control of red-green-blue photoluminescence in zeolites incorporated with rare-earth ions and a photosensitizer, *Angew. Chem. Int. Ed.* 45 (2006) 1925–1928.
- P.T. Jones, D. Geysen, Y. Tielemans, S. Van Passel, Y. Pontikes, B. Blanpain, M. Quaghebeur, N. Hoekstra, Enhanced Landfill Mining in view of multiple resource recovery: a critical review, *J. Clean. Prod.* 55 (2013) 45–55.
- D. Dupont, K. Binnemans, Rare-earth recycling using a functionalized ionic liquid for the selective dissolution and revalorization of $\text{Y}_2\text{O}_3\text{:Eu}^{3+}$ from lamp phosphor waste, *Green. Chem.* 17 (2015) 856–868.
- K. Binnemans, P.T. Jones, B. Blanpain, T. Van Gerven, Y. Yang, A. Walton, M. Buchert, Recycling of rare earths: a critical review, *J. Clean. Prod.* 51 (2013) 1–22.
- T. Aitasalo, J. Holsa, M. Lastusaari, J. Legendziewicz, J. Niittikoski, Persistent luminescence of Eu^{2+} doped alkaline earth aluminates MAL_2O_4 , *Radiat. Eff. Defect. Solids* 158 (2003) 89–96.
- S. Kundu, A. Kar, A. Patra, Morphology dependent luminescence properties of rare-earth doped lanthanum fluoride hierarchical microstructures, *J. Lumin.* 132 (2012) 1400–1406.
- M.M. Haque, H.-I. Lee, D.-K. Kim, Luminescent properties of Eu^{3+} -activated molybdate-based novel red-emitting phosphors for LEDs, *J. Alloy. Compd.* 481 (2009) 792–796.
- K. Binnemans, Lanthanide-based luminescent hybrid materials, *Chem. Rev.* 109 (2009) 4283–4374.
- I.C. Chen, T.-M. Chen, Sol-gel synthesis and the effect of boron addition on the phosphorescent properties of $\text{SrAl}_2\text{O}_4\text{:Eu}^{2+}, \text{Dy}^{3+}$ phosphors, *J. Mater. Res.* 16 (2001), pp. 644–651.
- O.L. Malta, H.F. Brito, J.F.S. Menezes, F.R.G. Silva, S. Alves, F.S. Farias, A.V.M. Andrade, Spectroscopic properties of a new light-converting device Eu(thenoyl-trifluoroacetate)₃ 2(dibenzyl sulfoxide). A theoretical analysis based on structural data obtained from a sparkle model, *J. Lumin.* 75 (1997) 255–268.
- O.L. Malta, H.F. Brito, J.F.S. Menezes, F.R. Gonçalves e Silva, C. de Mello Donega, S. Alves Jr., Experimental and theoretical emission quantum yield in the compound Eu(thenoyltrifluoroacetate)3.2(dibenzyl sulfoxide), *Chem. Phys. Lett.* 282 (1998) 233–238.
- R. Zhou, Q. Zhao, K.-K. Liu, Y.-J. Lu, L. Dong, C.-X. Shan, Europium-decorated ZnO quantum dots as a fluorescent sensor for the detection of an anthrax biomarker, *J. Mater. Chem. C* 5 (2017) 1685–1691.
- N. Chen, Y. He, G. Du, Preparation and luminescence of europium-doped lanthanum fluoride-benzoic acid hybrid nanostructures, *Mater. Sci. Semicond. Proc.* 24 (2014) 62–67.
- T. Matsuzawa, Y. Aoki, N. Takeuchi, A new long phosphorescent phosphor with high brightness, *J. Electrochem. Soc.* 143 (1996) 2670–2673.
- L.R. Melby, N.J. Rose, E. Abramson, J.C. Cari, Synthesis and fluorescence of some trivalent lanthanide complexes, *J. Am. Chem. Soc.* 86 (1964) 5117–5125.
- Z. Fu, L. Ma, S. Sahi, R. Hall, W. Chen, Influence of doping concentration on valence states of europium in $\text{SrAl}_2\text{O}_4\text{:Eu}$ phosphors, *J. Lumin.* 143 (2013) 657–662.
- M.H. Kostova, C. Zollfrank, M. Batentschuk, F. Goetz-Neunhoffer, A. Winnacker, P. Greil, Bioinspired Design of $\text{SrAl}_2\text{O}_4\text{:Eu}^{2+}$ Phosphor, *Adv. Funct. Mater.* 19 (2009) 599–603.
- D.S. Kshatri, A. Khare, Comparative study of optical and structural properties of micro- and nanocrystalline $\text{SrAl}_2\text{O}_4\text{:Eu}^{2+}, \text{Dy}^{3+}$ phosphors, *J. Lumin.* 155 (2014) 257–268.
- X. Zhang, S. Wen, S. Hu, L. Zhang, L. Liu, Electrospinning preparation and luminescence properties of $\text{Eu}(\text{TTA})_3\text{phen/polystyrene}$ composite nanofibers, *J. Rare Earths* 28 (2010) 333–339.
- Lianhui Wang, W. Wang, Wengong Zhang, A. Entang Kang, W. Huang, Synthesis and luminescence properties of novel eu-containing copolymers consisting of Eu(III)–Acrylate– β -Diketone complex monomers and methyl methacrylate, *Chem. Mater.* 12 (2000) 2212–2218.
- Q. Liu, D.M. Wang, Y.Y. Li, M. Yan, Q. Wei, B. Du, Synthesis and luminescent properties of $\text{Eu}(\text{TTA})_3\cdot 3\text{H}_2\text{O}$ nanocrystallines, *Luminescence* 25 (2010) 307–310.
- H. Chen, W. Zhang, Synthesis and characterization of a strong-fluorescent Eu-containing hydroxalate-like compound, *Sci. China Chem.* 53 (2010) 1273–1280.
- Q. Chen, S. Zheng, C. Huang, W. Zhang, Study on preparation and fluorescence characteristic of coordinated Eu_2O_3 /polymer hybrid films, *Appl. Surf. Sci.* 254 (2008) 5304–5313.
- E. Smecca, C. Tudisco, A.E. Giuffrida, M.R. Catalano, A. Speghini, G. Malandrino, G.G. Condorelli, Spatially confined functionalization of transparent NiO thin films with a luminescent (1,10Phenanthroline)-tris(2-thenoyltrifluoroacetate) europium monolayer, *Eur. J. Inorg. Chem.* 2015 (2015) 1261–1268.
- R. Zhang, G. Han, L. Zhang, B. Yang, Gel combustion synthesis and luminescence properties of nanoparticles of monoclinic $\text{SrAl}_2\text{O}_4\text{:Eu}^{2+}, \text{Dy}^{3+}$, *Mater. Chem. Phys.* 113 (2009) 255–259.
- H. Jeong, B.I. Lee, S.H. Byeon, Antenna effect on the organic spacer-modified eu-doped layered gadolinium hydroxide for the detection of vanadate ions over a wide pH range, *ACS Appl. Mater. Inter.* 8 (2016) 10946–10953.
- B. Gao, L. Fang, R. Zhang, J. Men, Preparation of aromatic carboxylic acid-functionalized polysulfone and preliminary exploration of fluorescence emission character of formed polymer-rare earth complexes, *Synth. Met.* 162 (2012) 503–510.